

A measurement of two-photon effects in unpolarized elastic electron-proton scattering

J. Arrington (Spokesperson), D. F. Geesaman, K. Hafidi, R. J. Holt, H. E. Jackson, D. H. Potterveld, P. E. Reimer, E. C. Schulte, X. Zheng
Argonne National Laboratory, Argonne, IL

M. E. Christy, C. E. Keppel
Hampton University, Hampton, VA

G. Niculescu, I. Niculescu
James Madison University, Harrisonburg, VA

R. Ent, D. Gaskell, A. F. Lung, D. J. Mack, D. G. Meekins
Jefferson Laboratory, Newport News, VA

R. E. Segel, I. Qattan
Northwestern University, Evanston, IL

R. Asaturyan, H. Mkrtchyan, V. Tadevosyan, T. Navasardyan
Yerevan Physics Institute, Armenia

(Dated: December 2, 2003)

Abstract

We propose a high precision measurement of the linearity of the Rosenbluth plot for elastic electron-proton scattering. Deviations from linearity are expected if there are sizable two-photon corrections, as has been proposed as an explanation of the discrepancy between Rosenbluth and polarization transfer measurements of the proton form factors. This measurement will provide a significant increase in the sensitivity to deviations from linearity. Based on estimates of the two-photon exchange terms, we expect that the measurement will be able to observe linearities at more than four standard deviations, or else set limits tight enough that the nonlinearities have no impact on the extraction of the form factors from a combined analysis of Rosenbluth and polarization transfer data.

I. INTRODUCTION

The structure of the proton is a matter of universal interest in nuclear and particle physics. Charge and current distributions are related to the electric and magnetic form factors, G_E and G_M , and so it is important to determine these quantities as accurately as possible. Recent polarization transfer measurements of the proton electromagnetic form factors [1–3] have led to significant new activity in modeling of the proton structure. Several new pictures have emerged, highlighting the role of relativity and angular momentum, and the ‘shape’ of the proton (For a review of the theoretical work, as well as details of the experiment, see Ref. [4]). However, these new measurements are in significant disagreement with previous extractions of the form factors that utilized the Rosenbluth separation technique (Fig. 1). Until we adequately understand the discrepancy between the experiments, we cannot be completely confident in our knowledge of the form factors, or the conclusions drawn from them about the role of relativity and quark angular momentum in the proton.

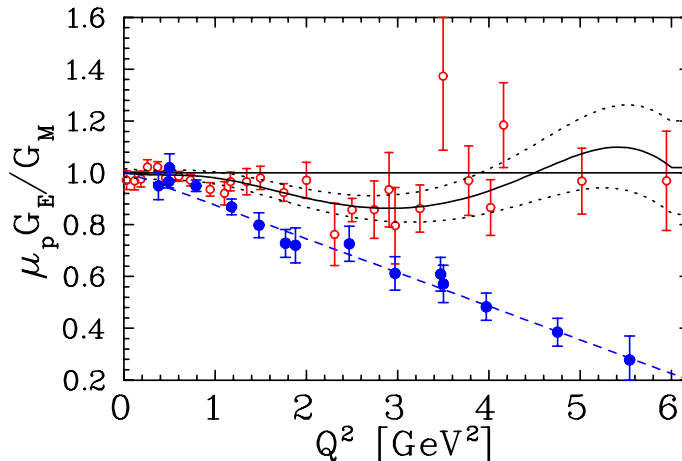


FIG. 1: $\mu_p G_E/G_M$ as deduced from a global Rosenbluth analysis [5] (open circles) compared to the polarization transfer extractions from [1, 2, 6] (filled circles).

In addition to the implications of the polarization transfer data on the structure of the proton, precise knowledge of the form factors is also important for many other experiments. The elastic cross section is often used as a check of experimental normalizations, and the difference between the Rosenbluth form factors and those extracted from polarization transfer could conceivably have significant impact on the normalization of several experiments. There are also many cases where knowledge of the electron-proton cross section is assumed when extracting information on nuclear structure. In quasielastic scattering from nuclei, the elastic cross section, parameterized by the form factors, is often removed from the measured cross section in order to access information on the proton distribution in nuclei. Errors in the form factors could have a significant impact on such experiments. Because the difference in form factors leads to a large difference in the ε -dependence of the cross section, these effects could be extremely important in cases where the ε -dependence is investigated [7]. Thus, the implications of the discrepancy are not limited to the structure of the proton, as there are several experimental results where a change in the form factors could have a direct or indirect impact on the extracted results.

Because of the difficulty in performing Rosenbluth extractions at large Q^2 , and apparent inconsistencies between different Rosenbluth experiments, it was argued that the discrepancy

was due to experimental problems in the Rosenbluth extraction. However, the systematic uncertainties of both the Rosenbluth [8] and polarization transfer [4] measurements have been studied in detail, and no explanation for the discrepancy in terms of experimental problems has been found. In addition, while the traditional Rosenbluth separation measurements are very sensitive to systematic uncertainties at large Q^2 , a recent ‘‘Super-Rosenbluth’’ measurement [9] was performed in Hall A, which is significantly less sensitive to the dominant sources of uncertainty in the traditional Rosenbluth measurements. Preliminary results from this experiment indicate good agreement with previous Rosenbluth measurements. This indicates that the discrepancy is not due to errors in the experiments or analyses, and that it may indicate a more fundamental problem with one of the techniques.

If the discrepancy is related to a fundamental problem with one (or both) techniques for extracting the form factors, rather than a simple experimental error, it is more difficult to know which technique is correct without some understanding of the source of the discrepancy. However, it does indicate that the discrepancy is unlikely to have a significant impact on other experiments. An uncertainty in the form factors, and thus the elastic cross section, could affect experiments which rely on knowledge of the cross sections as a calibration or normalization tool. Even if the discrepancy is caused by missing corrections to the cross section extraction, *e.g.*, two-photon corrections, the Rosenbluth extraction of the form factors is a direct fit to the *measured* cross sections. While the linear form implied by the Rosenbluth formula may not be exact, or the slope may not be equal to G_E^2 , it still provides a direct fit to the cross section. Thus, even if the Rosenbluth form factors are incorrect, they still provide a good parametrization of the cross section, appropriate for input in analysis of scattering experiments. In fact, they provide a much better parameterization for the cross section than the ‘true’ form factors, derived from polarization transfer data, unless the missing corrections to the cross section are understood [5].

Analyses of the discrepancy that assume the difference is due primarily to missing corrections in the cross section measurements [5, 8, 10, 11] indicate that the discrepancy could be explained by an error in the ε -dependence of the cross section of approximately 5–8% for $1 < Q^2 < 6 \text{ GeV}^2$. Coulomb corrections, when implemented in a simple effective momentum approximation [8, 12], do modify the ε -dependence of the cross section, but yield a very small effect compared to the size needed to explain the discrepancy. For the most part, investigations have focussed on the effect of two-photon exchange corrections [10, 13–15] beyond those included in the traditional calculations of radiative corrections [16–18].

One way to look for two-photon effects in the unpolarized cross section is to look for deviations from linearity in the ε -dependence of the reduced cross section. We propose a measurement that will have significantly greater sensitivity to two-photon effects in the linearity of the ε -dependence: a factor of six increase in the sensitivity over published measurements, and a factor of three over than projected results from E01-001 [9]. Based on estimates of the nonlinearities, discussed in Section III, the sensitivity should be enough to see these effects at the four sigma level.

Finally, the uncertainty in the extracted form factors can be resolved *without* a complete understanding of the two-photon corrections. Given a simple set of assumptions about the two-photon corrections, along with adequate Rosenbluth and polarization transfer data, we can extract the effect of two-photon exchange from the discrepancy. This has already been done [5, 11], but checks on the assumptions, as well as improved data to better measure the difference between the two techniques, are needed. This proposal will address two of these issues by directly testing the assumption of linearity in the correction, and by providing

improved Rosenbluth measurements of G_E/G_M in the region where the current data are not precise enough to extract two-photon contributions. Any observed nonlinearity can be incorporated into these extractions, and if we do not observe nonlinearities, then we know that the assumption of linearity in the extraction will not cause significant uncertainties in the extracted form factors.

There are two main goals for this proposal. First, we will perform a high precision test of the linearity of the Rosenbluth separation, sensitive enough to detect nonlinearities, estimated from current calculations, at the four sigma level. The data will constrain and test models of the two-photon effects on the unpolarized cross section. They will also determine the ε -dependence of two-photon corrections with enough precision that the *size* of the two-photon corrections can be extracted from the difference between Rosenbluth and polarization transfer measurements of the form factors, which will in turn allow an extraction of the proton form factors without the current uncertainties related to the assumptions about the form of the two-photon corrections. Second, we will provide several high precision Rosenbluth measurements of G_E/G_M . Coupled with the existing polarization transfer data, this will allow us to extract the size of the two-photon corrections for lower Q^2 values, where the current uncertainties on the Rosenbluth separation measurements make it difficult to determine the size of any discrepancy.

The above discussion assumes that two-photon corrections are responsible for the discrepancy. There are calculations [13, 15] that support this idea, as well as data from positron-proton elastic scattering [19]. If it turns out that the discrepancy is not related to problems with the cross section extractions, then the linearity measurement still significantly improves limits on two-photon (or other nonlinear) contributions, while the extractions of G_E/G_M provide a significant improvement in the extraction of proton form factors for $1 \lesssim Q^2 \lesssim 4 \text{ GeV}^2$.

II. SIGNATURES OF TWO-PHOTON EXCHANGE CONTRIBUTIONS

Two-photon exchange contributions to elastic electron-proton scattering can be observed in several different ways. The reactions can be broken down into two categories: polarization reactions, which are sensitive to the imaginary part of the two-photon amplitude, and unpolarized electron-proton scattering, which is sensitive to the real part. Spin observables, in particular those which are zero in the one-photon exchange approximation, can be used to cleanly isolate two-photon contributions. However, these measurements can be technically challenging. In addition, they are related to the imaginary part of the two-photon amplitude, and so are not directly connected to the modification of the unpolarized cross section, which may be responsible for the discrepancy in the proton form factor extractions.

There are two ways to look for the effects of two-photon corrections in the *unpolarized* elastic e-p cross section. First, one can compare positron-proton and electron-proton scattering. Interference terms between one-photon and two-photon exchange will have the opposite sign for positron-electron scattering, and will lead to a difference in the electron and positron cross sections. Such measurements require a precise comparison of positron and electron scattering, and have been limited by the luminosity of the secondary positron beams used for such measurements. Additional comparisons of positron to electron scattering over a range in Q^2 and ε would provide the most direct extraction of these two-photon corrections, but there is no facility where such measurements could be performed with the precision needed to map out these corrections over the necessary kinematic range.

Alternatively, one can test the linearity of the reduced cross section as a function of ε .

In the Born approximation, the reduced cross section should be a linear function of ε , and deviations from linearity would indicate a correction to the Born approximation that is not taken into account in the radiative corrections. This is not as direct a measurement as the comparison of positron to electron scattering, but it is sensitive to the nonlinear behavior of the two-photon contributions.

A. Experimental limits on nonlinearities

Several experiments have looked for two-photon exchange terms in the linearity of the Rosenbluth plot. Previous measurements have not shown any significant deviations from linearity, but have been limited by the size of the uncertainties and the ε range covered by most experiments.

To compare the proposed measurement to existing data, we need a figure of merit for the sensitivity to nonlinearities. We perform a quadratic fit to the ε -dependence of the data, and use the uncertainty of the quadratic term, (P_2 in Eq. 1), as an indication of the sensitivity of a given dataset to nonlinearities. For a quadratic fit centered on $\varepsilon = 0.5$,

$$\sigma_R = P_0(1 + P_1(\varepsilon - 0.5) + P_2(\varepsilon - 0.5)^2) \quad (1)$$

it is easy to see the size of the nonlinearities. For this parameterization, the fractional deviations from linearity are approximately $P_2(\varepsilon - 0.5)^2$, yielding $P_2/4$ at $\varepsilon = 0$ or 1 . Previous measurements have found P_2 to be consistent with zero, with $\delta P_2 > 0.10$. This yields limits on nonlinearities of $\sim 2.5\%$. However, this assumes that the nonlinearity is symmetric about $\varepsilon = 0$, and the data provide weaker limits if the nonlinearities occur only at large (or small) ε values. In addition, for a non-quadratic ε -dependence, the *size* of the extracted curvature parameter will depend on the ε range covered. The proposed measurement will dramatically reduce the uncertainties on P_2 , yielding an uncertainty of $\delta P_2 < 0.02$.

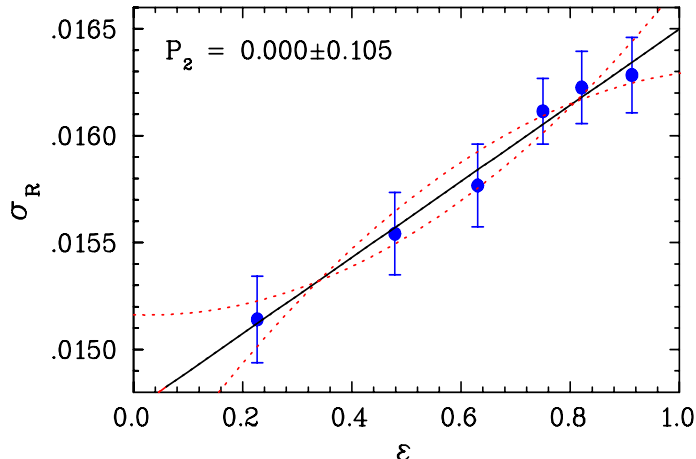


FIG. 2: The ε -dependence of the reduced cross section from NE11 (using only the data from the 8 GeV spectrometer). The solid line is the linear fit, while the dashed lines are quadratic fits with $P_2 = \pm 0.105$ (one-sigma variations from the central value).

The best extraction of the ε -dependence at large Q^2 is from SLAC NE11 [20] (Fig. 2). At $Q^2 = 2.5 \text{ GeV}^2$, the NE11 measurement took data at six ε values between 0.22 and

0.91, with uncertainties of 1-1.5%. The data are linear, and the uncertainty on P_2 is 0.105. The measurement by Walker, *et al.*, [21] did not have data below $\varepsilon = 0.6$, while the recent JLab E94-110 measurement [22], which was designed to perform L-T separation over the resonance region, does not have enough ε points at a given Q^2 value to set strong limits. By combining their data over a range in Q^2 , 2.5–3.5 GeV², there is enough ε range, and the uncertainty on the quadratic terms is similar to the NE11 limit, though for somewhat larger Q^2 . Similar limits can be placed on nonlinearities at lower Q^2 from Berger, *et al.* [23]. They measured the linearity of the Rosenbluth plot at several Q^2 values below 1 GeV², and found P_2 to be consistent with zero, with uncertainties that varied between 0.12 and 0.25 for $Q^2 \approx 0.4, 0.6, 0.8$, and 1.0 GeV².

One can attempt to combine different experiments in a global analysis to increase the sensitivity to small nonlinearities. However, while uncertainties in the overall normalization drop out when examining a single dataset, this is not true in a combined analysis of multiple datasets. Including the normalization uncertainties, which are often larger than the ε -dependent uncertainties, greatly reduces the significance of the measurement. Typically, such global analyses use the consistency of the datasets in order to extract the relative normalizations of different experiments. However, this involves assuming a smooth Q^2 -dependence and a linear ε -dependence to compare datasets at different kinematics. Such an assumption will tend to mask any real nonlinearity, making it difficult to learn anything from a global analysis.

E01-001 [9] will provide an improved limit on nonlinearities. At $Q^2 = 2.64$ GeV², there are five points for $0.12 < \varepsilon < 0.87$. The projected uncertainties in the E01-001 proposal are approximately 0.8%, which lead to an uncertainty of in P_2 of 0.064 (Fig. 6), nearly a factor of two better than previous measurements. The final results may yield $\delta P_2 \approx 0.05$, as the uncertainties may be smaller than projected in the proposal, and because any systematics that are purely linear in ε will not contribute to the uncertainty in extracting nonlinearities. However, the ε range of the data, and the limited number of ε points taken (five for $Q^2=2.64$ GeV², less for the higher Q^2 values) limit the sensitivity of the E01-001 measurement.

B. Positron to electron comparisons

There have also been several measurements comparing positron-proton scattering to electron-proton scattering. For positron-proton scattering, the interference between the one-photon and two-photon amplitudes changes sign, yielding a ratio $R \equiv \sigma(e^+p)/\sigma(e^-p) \approx 1 + 4\text{Re}(B/A)$, where B is the two-photon amplitude, and A is the one-photon amplitude. The modification to the electron cross section is approximately $1 - 2\text{Re}(B/A)$, and so a two-photon correction to the electron cross section will yield roughly twice the change in R , but with the opposite sign. In the simplest approximation, one expects the two-photon amplitude to be suppressed by an additional factor of α , leading to a decrease of $2\alpha \approx 1.5\%$ in the electron cross section, and an increase of $4\alpha \approx 3\%$ in the ratio R .

Additional differences come from Bremsstrahlung corrections when proton recoil is taken into account, but these are included in the usual radiative corrections, and have thus been corrected for in previous measurements. An analysis by Mar and collaborators [24] found these corrections to be relatively small, typically 1–2% for their kinematics, and to be identical to better than 0.3% in different prescriptions [18, 25] of the radiative corrections.

Figure 3 shows the existing data [24, 26–32] for the ratio of positron-proton to electron-

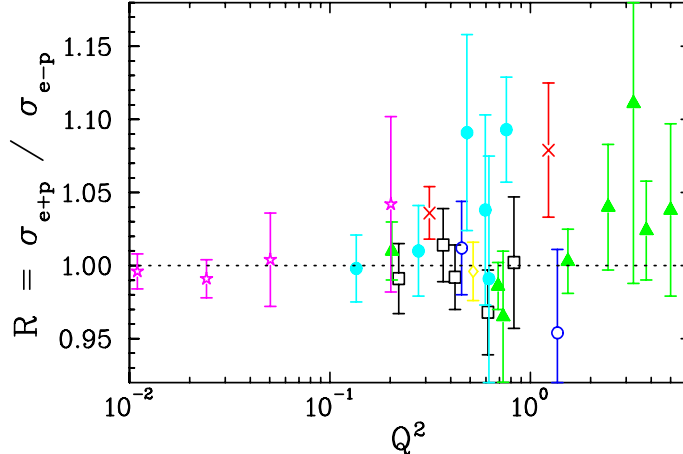


FIG. 3: $\sigma_{e^+}/\sigma_{e^-}$ cross section ratio as a function of Q^2 . The experiments are differentiated by color and symbol: black squares [26], red crosses [27], green solid triangles [24], blue hollow circles [28], yellow diamond [29], cyan filled circles [30], and magenta stars [31].

proton elastic cross sections as a function of Q^2 . The data yield $\langle R \rangle = 1.003 \pm 0.005$, with $\chi^2_\nu = 0.87$. This corresponds to a two-photon correction to the electron cross sections of $(-0.15 \pm 0.25)\%$. These data have been interpreted as showing that the two-photon corrections must be even smaller than the naive estimate, and thus limiting two-photon corrections to the electron-proton cross section to less than one percent.

A recent preprint [19] has reexamined the positron data, and shown that it is possible that two-photon effects could be large enough to explain the observed discrepancy, and yet be consistent with the limits set by the positron data. The discussion in this preprint is summarized here, as it demonstrates that the positron data support the idea of large two-photon exchange corrections. The positron data also provide information on the form of the two-photon correction, which when combined with the linearity measurement proposed here, will provide enough information on the ε -dependence of the two-photon corrections to allow a precise and accurate extraction of the proton form factors. Without adequate knowledge of the ε -dependence of the two-photon correction, there is an ambiguity associated with the assumptions made when combining the inconsistent results from polarization transfer and Rosenbluth measurements.

The low intensity of the secondary positron beams make precise measurements difficult in regions where the cross section is small. Because of this, all of the data in Fig. 3 are for low Q^2 ($Q^2 < 1.3 \text{ GeV}^2$) or small scattering angles ($\varepsilon > 0.7$). So while the existing data do place fairly tight limits on the size of two-photon corrections in some regions, two-photon effects are not constrained for large Q^2 , low ε values.

If we assume that two-photon corrections are responsible for the discrepancy between polarization transfer and Rosenbluth measurements, we can make specific predictions about how these corrections would affect the positron measurements. To explain the discrepancy, the effect must increase the slope of the Rosenbluth plot, and so must either increase electron the cross section at large ε or decrease the cross section at low ε . Based on the size and Q^2 -dependence of the discrepancy, the ε -dependence of the effect must be 5–8%, depending only weakly on Q^2 , for $Q^2 \gtrsim 2 \text{ GeV}^2$. It must also be reasonably close to linear in ε , or else it would introduce nonlinearities in the Rosenbluth plot. This implies that positron to electron ratio should have a 10–15% ε -dependence, approximately linear in ε , which increases the

ratio as small ε relative to large ε .

The positron data with a good ε range are limited to lower Q^2 values. In Fig. 4, the data for $Q^2 < 2 \text{ GeV}^2$ are plotted as a function of ε , and a significant ε -dependence can be seen. A linear fit, neglecting any Q^2 -dependence, yields an ε -dependence of $-(5.7 \pm 1.8)\%$, with $\chi^2 = 11$ for 22 degrees of freedom. The extremely small χ^2 indicates that at least some of the data have quoted overly conservative uncertainties. This may mean that the uncertainty in the slope is an overestimate, but there is no way to be sure without know which datasets have overly large estimates of their uncertainty.

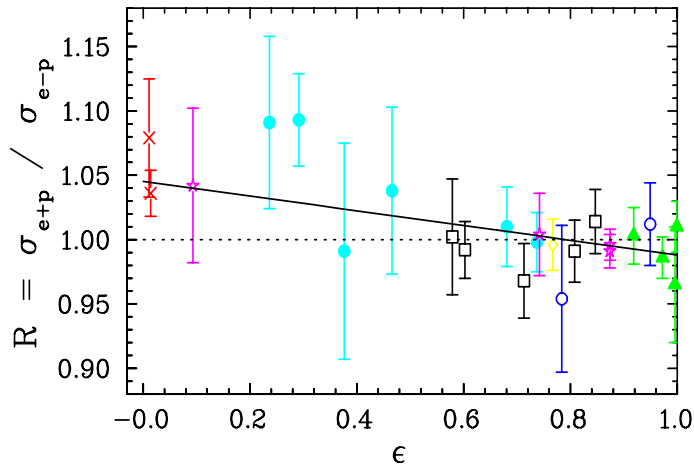


FIG. 4: The ratio $R = \sigma_{e+}/\sigma_{e-}$ as a function of ε for the measurements below $Q^2 = 2 \text{ GeV}^2$. The solid line is a fit assuming a linear ε -dependence and no Q^2 -dependence to the ratio, and yields a slope of $-(5.7 \pm 1.8)\%$. The symbols are identical to Fig. 3.

We can estimate the ε -dependence necessary to explain the discrepancy in the form factors at large Q^2 , but at these low Q^2 values the polarization transfer and Rosenbluth form factors are not precise enough to determine if there is an inconsistency, and so cannot be used to estimate the size of the two-photon corrections. At larger Q^2 values, where the size of the corrections can be estimated from the discrepancy, the ε -dependence for the electron cross section decreases somewhat as Q^2 decreases, and is approximately 5% for $Q^2 = 1\text{--}2 \text{ GeV}^2$. The correction must be smaller for very low Q^2 values ($0.01\text{--}0.1 \text{ GeV}^2$), or the decrease in the low- ε cross sections would yield to significant reductions in the extracted values of G_M . The extractions of G_M are not precise enough to conclude that the corrections must go to zero, but they must be significantly smaller than the 5% corrections observed at larger Q^2 values, implying that the ε -dependence in the positron to electron ratio must be less than 10% for $Q^2 < 1 \text{ GeV}^2$.

A global analysis of the cross section and polarization transfer data was used to try and estimate the low Q^2 behavior. In Ref. [5], a global analysis of the cross section and polarization transfer data, assuming a fixed 6% ε -dependent correction to the cross section, was used to extract the ‘Polarization form factors’. A modified version of this analysis was performed, but rather than extracting G_E and G_M with a fixed two-photon correction, we extracted G_E , G_M , and the Q^2 -dependence of the linear ε -corrections. Several different functional forms were tried, and a range of curves, which all give good fits, are shown in Fig. 5 as solid lines. The three dotted curves are additional parameterizations, fit to the high Q^2 extraction of Ref. [10], and using different function forms to extrapolate to lower

Q^2 . While the fits were not constrained to go to zero, they all yield a much smaller value as $Q^2 \rightarrow 0$. When these curves are used to estimate the ε -dependence for the positron data at $Q^2 = 0.4 \text{ GeV}^2$, they yield slopes of $-(3.6 - -7.0)\%$, consistent with the observed -5.7% slope.

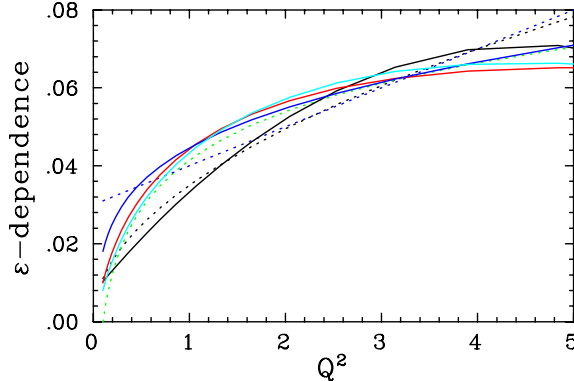


FIG. 5: The extracted size of the (linear) ε -dependence of the electron-proton cross section as a function of Q^2 , as determined from the difference between polarization transfer and Rosenbluth form factors. Because this can only be extracted with good precision at $Q^2 \gtrsim 2 \text{ GeV}^2$, several different forms are used to estimate the behavior at lower Q^2 values. The four solid curves correspond to four different parameterizations for the Q^2 -dependence, used in the global analysis of cross section and polarization transfer data. The three dotted lines are empirical fits to the extracted slopes at high Q^2 values from Ref. [10], using different forms for the Q^2 -dependence.

While we cannot make a direct comparison of the two-photon corrections implied by the positron measurement to those necessary to explain the form factor discrepancy, this data yield important information on these two-photon corrections. The observed ε -dependence in R provides evidence for large two-photon corrections in the elastic cross sections, and supports the idea that they may explain the discrepancy between polarization transfer and Rosenbluth separation measurements. In addition, the fact that the two-photon contributions are only large at low ε values puts significant constraints on the form of the corrections, and in fact already rules out some models where the discrepancy is explained by two-photon effects at large ε [10, 14]. If we combine this information with this proposed measurement of the nonlinearities (or tight enough upper limits on deviations from linearity) we can extract the form factors from a combined analysis of cross section and polarization data. The only remaining uncertainties in the combination of the data sets is associated with the size of two-photon corrections on the polarization transfer data, which are expected to be much smaller than for the unpolarized cross section measurement [10, 14, 15].

III. ESTIMATES OF THE TWO-PHOTON EXCHANGE CORRECTIONS

In the 1950s and 1960s, several papers estimated the size of two-photon contributions to the unpolarized cross sections, including only the unexcited intermediate proton state [33], or including excitations of the intermediate state [34–37]. In general, the predicted two-photon effects were consistent with the apparent lack of difference between positron and electron scattering, and were too small to introduce observable nonlinearities. Very recently, a significant amount of work has gone into improving such calculations [13, 15], or attempting

to make model-independent statements about the form of such corrections [10, 14]. All of the new calculations that provide predictions for the ε -dependence of the two-photon corrections yield noticeable nonlinearities. It has also been argued that there *must* be nonlinearities generated by the two-photon correction [14, 15].

Calculations by Blunden, Melnitchouk, and Tjon [13] yield an ε -dependence of $\approx 2\%$, with small nonlinearities at low ε values. With the inclusion of improved form factors, these corrections increase to $\approx 3\%$ [38]. This calculation yields almost no correction at $\varepsilon \approx 1$, and a decrease at low ε values, consistent with what is observed in the positron to electron ratios. However, these calculations include only the elastic portion of the two-photon correction, *i.e.* the box and crossed-box diagrams with the proton in the intermediate state, and neglect intermediate states which have been shown to be important in other processes in certain kinematic regimes [39, 40].

Calculations by Afanasev [15] yield a different form for the ε -dependence. Again, the two-photon correction is small at large ε values, and so is not ruled out by positron measurements, but it yields a very different nonlinearity than Ref [13]. Figure 6 shows the ε -dependence of these calculations, along with that of Rekaló and Tomasi-Gustafsson [14].

We use these calculations to estimate the size of possible nonlinearities in the ε -dependence. Ref. [14] provides only the form of the ε -dependence, and so this curve is normalized so that the overall change in slope is large enough to explain the observed discrepancy. The calculation of Ref. [13] gives the size of the effect as well as the ε -dependence, but includes only the contributions where the intermediate proton state is unexcited, and, even in their updated calculation only yields a 3% change in the slope. Therefore, to estimate nonlinearities we use their calculated ε -dependence but double the size of their correction, so that the correction explains the observed discrepancy.

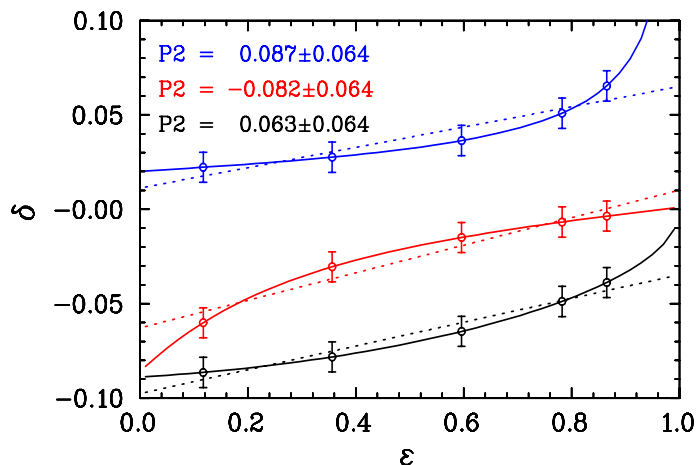


FIG. 6: The two-photon contributions to the elastic e-p cross section (δ is the fractional change to the cross section) from the updated calculations of Blunden, Melnitchouk, and Tjon [13, 38] (red (middle) curve), Afanasev [15] (black (bottom) curve), and Rekaló and Tomasi-Gustafsson [14] (blue (top) curve). The circles indicate the kinematics and uncertainties (at $Q^2 = 2.64 \text{ GeV}^2$) for the preliminary results of E01-001 [9], placed on each of the calculations. The dotted lines are linear fits to each set of E01-001 pseudo-data.

Using the quadratic (P_2) term of Eq. 1 to estimate nonlinearities, previous measurements have shown ε -dependence consistent with linear behavior, with large uncertainties on P_2

($\delta P_2 > 0.10$). Apart from the curve of based on Ref. [14], which is already ruled out by the positron measurements at large ε values, the curves are consistent with previous measurements of the nonlinearities of the Rosenbluth cross section and the comparisons of positron to electron scattering. The results from E01-001 [9] will provide improved limits, yielding $\delta P_2 \approx 0.60$. To estimate the sensitivity of these data to the estimated nonlinearities, the E01-001 points are placed on each of the curves, with the current uncertainties of the measurement. Figure 6 shows the points placed on calculations from Refs. [14] (top curve), [13] (middle curve), and [15] (bottom curve). While the final uncertainties for E01-001 measurement will be slightly smaller, the measurement would still provide a significance of less than two standard deviations for the two lower curves.

From Fig. 6, it is clear that the size of the extracted nonlinear term depends on the ε range covered, as the various calculations show nonlinearities in limited (but different) regions of ε . So depending on the form of the ε -dependence, the E01-001 data typically has sensitivity to nonlinearities only in one or two points. While the data have comparable ε -coverage and smaller uncertainties than previous measurements, they are still not sensitive enough to clearly see the estimated nonlinearities. For a precise measurement of the nonlinearities, it is important to minimize the uncertainties, cover the maximum possible ε range, and have several points at both large and small ε values, so that there will be several points in the linear region to act as a precise ‘baseline’ for nonlinearities.

IV. EXPERIMENT

The proposed measurement is a conventional Rosenbluth separation, but instead of detecting the scattered electron, we will detect the struck proton. Detecting the proton leads to a reduced cross section dependence on the kinematics (beam energy and scattering angle) and reduces several ε -dependent systematic uncertainties. The major sources of uncertainty in the most precise SLAC measurements [20, 21] were uncertainty in the scattering kinematics, the total charge, corrections that depended on rate or kinematics, and the target density. Because we measure the protons, we are less sensitive to knowledge of the scattering kinematics, and have a constant proton momentum. In addition, the cross section is nearly constant when detecting the proton, so that any rate-dependent corrections will yield minimal ε -dependence. It also means that we can use a constant beam current, reducing the relative uncertainty in accumulated charge and target density at different ε values.

The first goal of this proposal is to make an improved measurement of any nonlinearities in the ε -dependence. Current measurements of the curvature yield $\delta P_2 > 0.10$ for both small and moderate Q^2 values. The final projected uncertainties for E01-001 will be able to reduce this to 0.05–0.06 for $Q^2 = 2.64 \text{ GeV}^2$. The projected uncertainties for this proposal yield $\delta P_2 < 0.02$ for $Q^2 = 2.56$ and 1.12 GeV^2 . In addition to improving the uncertainty in the determination of P_2 , the *size* of the observed nonlinearity grows somewhat as the ε range increases for all of the curves shown in Fig. 6. By increasing the ε range of the data, the number of ε points, and reducing the ε -dependent systematics, we will have a sensitivity of four standard deviations to each of the forms shown in Fig 6, at two different Q^2 values. In addition, while the curvature of the quadratic fit is a useful general measure of the nonlinearities, we can provide better discrimination against specific models, and in some cases, improve our determination of nonlinear effects by independently analyzing the low ε data and the large ε data.

The second goal is to provide additional, high precision L-T separations for $1 \lesssim Q^2 \lesssim$

4 GeV², to allow a more precise ‘extraction’ of the two-photon effects from the discrepancy between Rosenbluth and polarization transfer measurements. Such a determination, necessary for a precise extraction of the proton form factors, must start with several assumptions. We must assume that the discrepancy comes from two-photon effects, and we must assume a functional form for the effect on both the polarization transfer and Rosenbluth data. The proposed measurement will provide the ε -dependence of the correction to the cross section data, either by measuring nonlinearities, or by setting tight limits that ensure that the effect of nonlinearities on such an extraction are negligible. The positron data give a strong indication that two-photon effects are responsible, and that these corrections are very small at large ε . With the combination of the positron data and the proposed measurement, we will determine the ε -dependence, and have precise data with which to extract the size of the two-photon corrections. The only remaining assumption in extracting the proton form factors is that the two-photon effects do not significantly modify the polarization transfer measurement. The high precision Rosenbluth data at lower Q^2 values will also allow a more direct comparison of the two-photon effects observed in positron scattering with those deduced from the discrepancy between Rosenbluth and polarization transfer form factor measurements.

A. Kinematics

A precise measurement of any nonlinearities will require taking data at many ε values, including several low and high ε points. This means taking data at several beam energies to get enough ε points, and using multiple linac settings in order to have sufficient measurements to be sensitive to nonlinearities at low ε . Figure 7 shows the kinematics (Q^2 vs. ε) for elastic scattering for some of the energies achievable with six proposed linac energy settings. The green lines correspond to $E_{linac}=887$ (solid), 942 (dashed), and 1002 (dotted) MeV per pass, while the light blue lines correspond to 1067 (solid), 1133 (dashed), and 1200 (dotted) MeV per pass. These are the linac energies required by E02-010, scaled up to reach a maximum energy of 6.0 GeV, rather than the 5.7 GeV in that proposal. This change is consistent with the requirements of E02-010 [41], although the measurement proposed here would not be significantly affected by running at slightly lower energies.

Using these linac energies, we can measure several ε points at both large and small ε -values for $Q^2=1.12$ and 2.56 GeV². For the low (high) Q^2 point, we will take one-pass (two-pass) data for each of the linac settings to provide six low ε points, and then take data at six more high ε values, spaced roughly uniformly up to the maximum possible value. This will also allow us to determine the slope in the linear region, and then see the effect of any nonlinearities in multiple data points. With a small amount of additional running time, we will make precise extractions of G_E/G_M at $Q^2=0.90, 1.42, 1.65,$ and 3.65 GeV², in addition to the points at $Q^2=1.12$ and 2.56 GeV².

B. Advantages of proton detection

For this measurement, proton detection has several advantages over electron detection. Table I compares the electron kinematics to the proton kinematics for the two Q^2 values where we propose to make precise linearity tests. If we were to detect the electron, we would have to go to extremely large scattering angles to obtain the small ε data. This

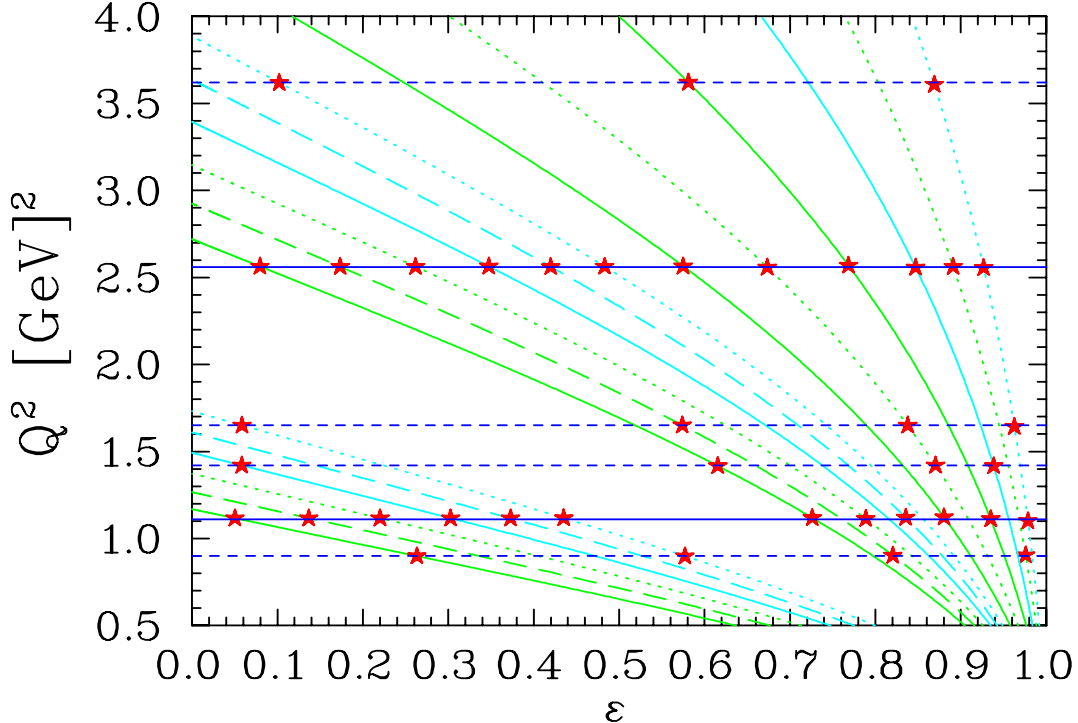


FIG. 7: The ε values that can be measured as a function of Q^2 for the available electron energies. The solid blue indicate the Q^2 values where the nonlinearity measurements will be performed (12 ε values each), while the dashed lines indicate the additional Q^2 values where we will make precise measurements of G_E/G_M . The red stars indicate the points where measurements will be taken. The minimum ε value is determined by the minimum scattering angle of 10.5 degrees.

means that we would have to detect electrons from roughly 300 MeV to more than 5 GeV, and so any momentum-dependence in the optics, detector efficiency, or particle identification would introduce an additional ε -dependence. For protons, the momentum at a fixed Q^2 is constant. In addition, at large electron angles the cross section is extremely small. The cross section for the proton is much less dependent on ε , leading to three significant advantages: (1) the minimum cross section is 10–20 times higher for the proton than for the electron, (2) the maximum cross section is much lower, meaning that any rate-dependent efficiency correction will be smaller and introduce less ε -dependence, and (3) the small variation of cross sections with ε means that we can run at fixed beam current, reducing the ε dependence of any corrections due to target heating or BCM nonlinearities.

The uncertainty in the scattering angle was one of the the largest sources of uncertainty in previous measurements (where the electron was detected). For our kinematics, the electron cross section can vary by up to 4.2% for a 1 mrad error in the scattering angle. For the proton, the size and ε -dependence of this correction are typically a factor of two smaller, and the ε -dependence is roughly linearly (Fig. 8). So not only is the correction due to a constant (beam or spectrometer) angle offset smaller by a factor of two or more, the deviations from linearity are even smaller. Finally, because the scattered electron is not detected, the radiative corrections are smaller.

There will be corrections to the absolute cross section that are larger when detecting the proton, but these are very nearly independent of ε . Protons will undergo hadronic reactions

	$Q^2 = 1.12 \text{ GeV}^2$ settings		$Q^2 = 2.56 \text{ GeV}^2$ settings	
	Proton	Electron	Proton	Electron
ε	0.05–0.98	0.05–0.98	0.08–0.93	0.08–0.93
p	1.21 GeV/c	0.34–5.47 GeV/c	2.10 GeV/c	0.46–4.70 GeV/c
θ	10.5–55.5°	10.5–139°	10.5–41.5°	17.2–123°
σ	3.9–9.5 nb/sr	0.3–110 nb/sr	0.30–0.52 nb/sr	0.014–1.93 nb/sr
$\Delta\sigma/\Delta\theta$	0.4–1.6 %/mr	-(0.1–4.2)%/mr	0.7–1.7 %/mr	-(0.1–2.8)%/mr

TABLE I: Comparison of electron and proton kinematics for the $Q^2=1.12 \text{ GeV}^2$ and $Q^2 = 2.56 \text{ GeV}^2$ measurements.

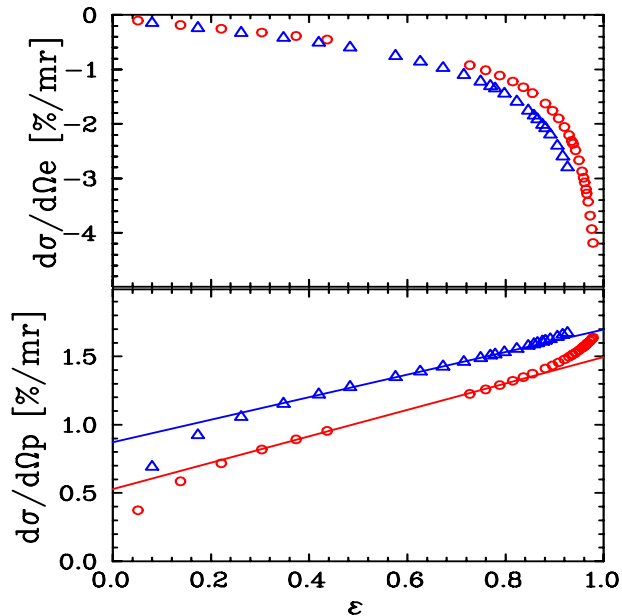


FIG. 8: Cross section-dependence on the scattering angle for detection of electrons (top) and protons (bottom). The red circles are for $Q^2 = 1.13 \text{ GeV}^2$, while the blue triangles are for 2.56 GeV^2 . The solid lines in the bottom figure show a linear fit over the intermediate ε range to show the deviations from linearity.

and be lost in the target or detector materials. This leads to a loss of $\sim 5\%$ of the protons, which depends mainly on the proton momentum. There is a small ε -dependence, because the amount of target material the proton interacts with changes as the proton angle changes. This variation is quite small, and is taken into account in the simulation of the experiment.

Protons are not always stopped by the HMS collimator, so one can not fully rely on the collimator to define the solid angle for the measurement. We will define the solid angle using cuts on the reconstructed scattering angles, in a region where the HMS has 100% acceptance. While any error in the angular reconstruction will lead to an uncertainty in the *absolute* solid angle, identical cuts will be used at forwards and backwards angle, and so essentially all of the uncertainty in the solid angle will cancel. The software cuts may yield an additional offset in the average scattering angle, but it will be the same offset for all settings, and because the effect of a fixed shift in the proton angle is nearly linear, the

effect on the linearity test is extremely small.

C. Backgrounds

The biggest drawback in detecting the protons is the presence of background processes that generate protons close to the elastic peak. Figure 9 shows proton singles spectra from E01-001, plotting the difference between the measured proton momentum and the momentum calculated from the measured angle, assuming elastic scattering. The elastic events peak near zero, and have a radiative tail (blue dots). These events sit on top of a significant background of events coming from the target endcaps (yellow points, largely covered by the magenta points which include the Compton scattering background). In addition, there are events from Compton scattering (magenta) and π^0 - p events from pion photoproduction (green).

The contributions from the target endcaps are a larger fraction of the elastic peak than in the case of electron detection, and include both electroproduction and photoproduction processes. We will take adequate measurements with an aluminum ‘dummy’ target, and use a target that more closely matches the radiation length of the hydrogen target in order to minimize the differences between the endcap and dummy target contributions. For E01-001, the endcap subtraction varies between 10% at high ε values to 25% at low ε values, for a cut on δp (plotted in Fig. 9) from -20 MeV to +40 MeV. This cut is quite wide because of the long non-gaussian tails in the elastic peak. These tails come from poor track reconstruction, which is currently being addressed in the E01-001 analysis, but which is not an issue for tracking with the HMS drift chambers. For the proposed measurement, this cut can be made tighter, reducing the background contribution by nearly a factor of two and yielding an ε -dependence of <10% in the background subtraction. We should be able to measure the endcap contribution to better than 3%, yielding an uncertainty in the slope of <0.3%, and contributions to the nonlinearity that are less than 0.1%.

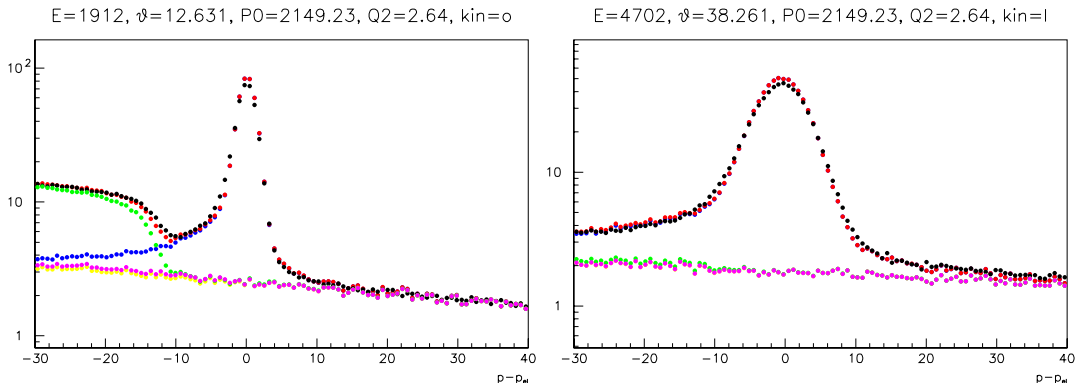


FIG. 9: HRS Proton elastic singles spectra from E01-001. The left plot is for the lowest ε point, and the right is for the higher ε point, both at $Q^2 = 2.64 \text{ GeV}^2$. The black dots are the data, the yellow are the dummy target data (scaled to match the endcap contributions), while the other points are the dummy data combined with the simulated Compton (magenta), $\pi^0 - p$ (green), and elastic (blue) simulations. The red points show the sum of the endcap data and all of the simulated processes.

Photoproduction of neutral pions is the other significant background of high energy protons. For the low Q^2 data, the threshold for pion production is far enough below the elastic peak that it can be easily cut away. For the higher Q^2 values, we will need to subtract away these contributions. Figure 9 shows a measured spectrum of proton elastic singles from a Hall A measurement at $Q^2 = 2.64 \text{ GeV}^2$, along with a Monte Carlo simulation of the contributions from elastic scattering from protons (smeared to reproduce the HRS resolution and non-gaussian tails), quasielastic scattering from the aluminum target windows, and protons coming from pion photoproduction (using $d\sigma/dt \propto s^{-7}$, and normalizing to the measured distribution). For a cut of $\delta p > -20 \text{ MeV}$, the pion photoproduction background is $\lesssim 10\%$ of the elastic yield, and is well reproduced by the calculated photoproduction spectrum. The contribution is largest for small ε values, where the δp resolution is best, and where we can vary the cut to compare a tight cut (excluding the background but sensitive to how well we reproduce the shape of the elastic peak) to a loose cut (insensitive to the resolution, but with larger background contributions). In addition, we will have coincidence runs at a few kinematics, which will allow us to separate the elastic and the photoproduction in order to test our calculations of the line shapes.

There will also be a background of charged pion photoproduction. For some kinematics the pion production threshold is far enough below the elastic peak to cleanly separate the pions. Time of flight will efficiently remove pions for the low Q^2 data, and an Aerogel detector will be used to reject pions where the time of flight is not fully efficient. The pion contamination will be negligible after the PID cuts, while the inefficiency of the cuts depends only on the pion momentum, which is fixed for fixed Q^2 values.

D. Experimental equipment

The experiment is proposed for Hall C using the HMS spectrometer and the standard cryogenic targets. The 4 cm liquid hydrogen target will be viewed at a maximum angle of 60 degrees, so target length effects on the acceptance will be negligible. An Aerogel detector will be used for p/π separation. Solid angles will be restricted to about 3.2 msr by software cuts. Coincidence data will be taken at a few of the kinematics, in order to check our modeling of the background and the resolution and radiative tail for the elastic peak.

E. Yields

A beam of $70 \mu\text{A}$ on a 4 cm liquid hydrogen target gives a luminosity of 7.6×10^{37} which, for a 3.2 msr solid angle, means that the expected yields can be obtained by multiplying the cross sections (in fm^2/sr) by 2.4×10^9 . This yields ~ 20 counts/second at the lowest yield point ($Q^2 = 3.65 \text{ GeV}^2$, lowest beam energy). The cross sections are a factor of three or more higher at all of the other Q^2 settings, so the desired statistics (0.1–0.2%) can be achieved in a few hours for each setting.

F. Systematic uncertainties

Because of the high precision required for this measurement, we have to ensure that we take into account many corrections that are often assumed to be small or negligible. Dead

time corrections, bin centering, and uncertainties in the kinematic quantities all have to be corrected for precisely.

Computer dead time corrections are measured in the standard data acquisition system in Hall C. The number of triggers generated and the number of events actually written to tape are recorded, and the cross section is corrected by the fraction of events sampled, with a very small associated uncertainty. Electronic dead time is determined by measuring the loss of events for a variety of electronic gate widths (starting at 50 ns, the nominal gate width for the trigger signals) and extrapolating back to zero gate width. A larger problem could be multiple tracks in the chambers. While the tracking code does a good job of selecting the track that formed the trigger, there can be confusion in the tracking for overlapping events. The time window over which this could cause problems is 200-300 ns.

At low Q^2 , the elastic rate over the full (~ 7 msr) solid angle varies from 4 kHz at low beam energy to 10 kHz at high beam energy. However, the inelastic backgrounds are larger at forward angles so the raw event rate, which determines deadtime and tracking inefficiencies, should vary by less than a factor of two. The maximum rate will be less than 20 kHz, leading to electronic deadtime and multiple track corrections below one percent, with an ε -dependence that is less than half of this size. The uncertainties on these corrections will be less than 0.1%. At larger Q^2 values, the trigger rate is dominated by the inelastic contribution, and decreases with scattering angle. However, the maximum rates should be 5 kHz or less, making the uncertainty in the ε -dependence of these corrections negligible.

Our estimates assume that we will accept protons over a ± 20 mr angular range in scattering angle. Because the cross section is not constant over this range, we will need to apply a bin centering correction to extract the cross section at the central scattering angle. The cross sections can vary significantly over the measured range, but the bin centering correction is quite small because over the 40 mr acceptance, the cross section is nearly linear and the acceptance is flat. Simulations of elastic scattering at each of the kinematics, including both the cross section variation and HMS acceptance, show extremely small bin centering corrections, and indicate that the uncertainty in the bin centering correction we apply is $< 0.1\%$.

Significant systematic uncertainties can come from the uncertainty in the scattering kinematics. The sensitivity of the cross sections is typically 4–6% for a one percent change in beam energy, with little ε -dependence. So an overall scale uncertainty in the beam energy has almost no effect on the ε -dependence. This measurement is more sensitive to uncorrelated beam uncertainties. Assuming a point-to-point beam energy uncertainty of 0.04%, as obtained by E94-110 [42], the cross sections vary by about 0.2%.

The uncertainty in the angle of the scattered proton also breaks down into an overall offset (identical for both forward and backward angles) and an offset that can vary randomly as the spectrometer angle is changed. The overall offset has contributions from both the incoming beam angle and any offsets in the spectrometer angle. In addition, because we will define the scattering angle acceptance with software cuts rather than with a collimator, an error in the angle reconstruction will modify the size and central angle for the defined angular acceptance. We will use the same cuts for all kinematics and so the uncertainty in the total solid angle will cancel, but there can still be an overall offset in the central scattering angle of the software restricted window. We expect to achieve an overall offset of 0.3 mr, higher than the 0.2 mr achieved in E94-110 due to the additional uncertainty associated with the software-defined solid angle. As seen in Fig. 8, a fixed offset yields a change in slope of $\approx 1\%$ per mr, but deviations from linearity of only 0.2% per mr. So a fixed 0.3 mr offset yields

a linear ε -dependence of 0.3%, which contributes to the uncertainty in G_E/G_M , but yields systematic deviations from linearity of $<0.1\%$.

Offsets that vary randomly with changing scattering angle come from any shifts of the drift chamber position during the run, as well as uncertainty in the pointing of the spectrometer and target position. At each angular setting the spectrometers will be surveyed and also data taken with a carbon target, attached to the cryotarget ladder, in order to verify the stability of the target position. Previous measurement [42] have achieved point-to-point uncertainties in the scattering angle of 0.2 mr. The sensitivity to the proton angle varies from 0.5–1.5% per mr, yielding uncertainties in the cross section of 0.1–0.3%.

G. Run plan

Data will be taken on 4 cm LH2 and aluminum ‘dummy’ targets for endcap subtraction. In addition to the proton inclusive data for the G_E/G_M measurement, we will take several test measurements. Runs will be taken at different beam currents in order to verify our measurement of the dead time and other rate-dependent effects in the spectrometers. Data will be taken with a thin carbon target at all kinematics as a check on the spectrometer pointing and target position. Finally, because we define the kinematics by the proton angle, we can use the measured proton momentum as a check on the kinematics. While for a single setting, it is not possible to disentangle a momentum offset from a scattering angle offset, the magnet settings stay the same when the scattering angle is changed, and so any momentum offset will be identical at all ε points for a given Q^2 . This will allow us to use the reconstructed momentum as an additional check on the kinematics.

Finally, coincidence data will be taken at some energies as a check of the scattering kinematics, and as a measure of proton detection efficiency and absorption (though these corrections almost completely cancel in the ε -dependence). Comparing the elastic cross section as measured by the protons and the electrons at one kinematics allows us to measure the proton inefficiency (due mainly to absorption). By comparing electron singles to proton singles at multiple kinematics (with a fixed proton momentum), we can also check the radiative corrections, which are significantly different for electron and proton singles. We can also use the coincidence data to examine the elastic proton spectrum without the backgrounds, allowing us to check the agreement between the data and the simulated elastic (and background) spectra.

Data taking for the points shown in Fig. 7 will require approximately four hours of running for each point at 3.65 GeV² (12 hours), three hours for each setting at 2.56 GeV² (36 hours), 1.5 hours for each setting at 1.12 GeV² (18 hours), and 1.5 hours each for the other points below 2 GeV² (18 hours). The time listed above includes running on the dummy target. We will also require 24 hours for coincidence runs, sieve slit runs, BCM calibration runs, and target boiling studies, for a total running time of 108 hours.

We require a total of 5 linac energy changes (8 hours each), and 12 additional pass changes (4 hours each), for a total time of 88 hours. The overhead assumed is very close to what was assumed by E02-010, which assumed 6 hours per energy change, but had 6 linac changes with only additional 9 pass changes. An additional 12 hours is requested for checkout and calibration. Thus, the total beam time request is 208 hours, or 9 days of beam time.

Source	Size	$\delta\sigma/\sigma$ total	$\delta\sigma/\sigma$ G_E/G_M	$\delta\sigma/\sigma$ linearity
Statistics	0.1–0.2%	0.1–0.2%	0.1–0.2%	0.1–0.2%
Energy (fixed offset)	0.04%	0.2%	<0.1% *0.1%	<0.1%
Energy (random)	0.04%	0.2%	0.2%	0.2%
θ_p (fixed offset)	0.30 mr	0.2–0.5%	0.1% *0.3%	<0.1%
θ_p (random)	0.20 mr	0.1–0.3%	0.1%	0.1–0.3%
Dead Time		0.1%	<0.1%	<0.1%
Dummy Subtraction		0.2–0.5%	0.2% *0.2%	<0.1%
Radiative Corrections		1.2%	0.2% *0.2%	~0.2%
Bin Centering		0.1%	<0.1%	<0.1%
Luminosity		0.5%	0.2%	0.1%
Proton absorption		1.0%	<0.1%	<0.1%
#Acceptance		~3%	<0.1%	<0.1%
#Efficiency		0.5%	<0.1%	<0.1%
Total		3.5%	0.53% *0.42%	0.36–0.46%

* Uncertainty given is on the slope rather than the individual cross sections

TABLE II: Projected uncertainties for the proposed measurement. These estimates allow for a small random fluctuation for those corrections which we expect will entirely cancel between the forwards and backwards angle (those marked with ‘#’). The error on the extracted G_E/G_M depends on the value of G_E/G_M .

H. Projected Data

Table II shows the projected uncertainties for the measurements. Separate entries are given for the total uncertainty in the individual cross sections, the uncertainties that enter into the extraction of G_E/G_M (neglecting uncertainties that are ε -independent), and the uncertainties that enter into the linearity tests (neglecting the portions of the systematic uncertainties that vary linearly with ε). Figure 10 shows the data points for the linearity checks, along with the projected uncertainties, placed on different estimates of the two-photon corrections as described in section III. For the $Q^2 = 2.64 \text{ GeV}^2$ measurement, the uncertainty on the quadratic term (P_2 from Eq. 1) is 0.018, which yields a 4.4σ measurement using the estimate based on the calculation of Blunden, Melnitchouk, and Tjon [13], and a 3.8σ measurement using the estimate of Afanasev [15]. For the $Q^2 = 1.12 \text{ GeV}^2$ measurement, $\delta P_2 = 0.017$, and P_2 is four or more standard deviation from zero for both estimates.

Figure 11 shows the projected uncertainties for the measurements of G_E/G_M , compared to existing Rosenbluth and polarization transfer data, and the current (and projected) un-

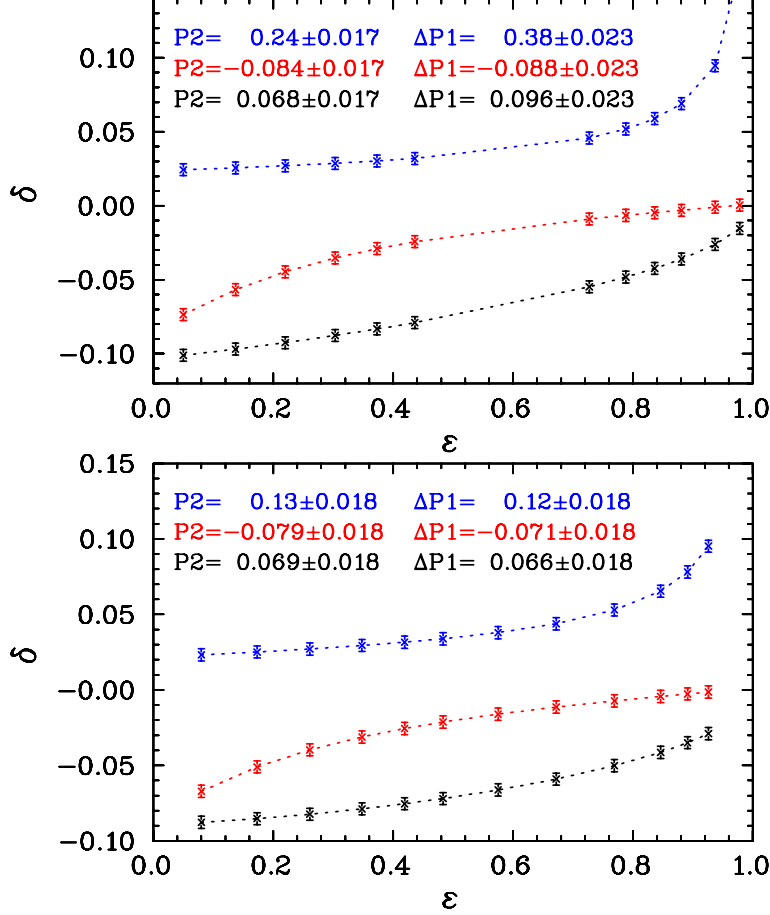


FIG. 10: The ϵ -dependence of the two-photon contributions to the elastic e-p cross section from calculations by Blunden, Melnitchouk, and Tjon [13] (red), Afanasev [15] (black), and Rekaló and Tomasi-Gustafsson [14] (blue). The crosses show the approximate kinematics and projected uncertainties (0.4%) for the proposed $Q^2 = 1.12 \text{ GeV}^2$ measurement (top) and the $Q^2 = 2.65 \text{ GeV}^2$ (bottom). For each curve, the extracted P_2 and its uncertainty are also shown. Because of the separation between the low and high ϵ points for the lower Q^2 data, the difference between the slope for the low ϵ and high ϵ points (ΔP_1) can also be used as a measure of deviations from linearity.

certainties for the preliminary results of E01-001. In addition to the significant improvement in the measurement of nonlinearities, these data will also significantly improve Rosenbluth extractions of G_E/G_M . This, coupled with the reduced systematic uncertainties in the final analysis of the polarization transfer measurement [4], will allow us to extract the size of the two-photon corrections, assuming that they explain the discrepancy between the two techniques. When good calculations of the two-photon corrections become available, these data will provide the most precise measurements of G_E/G_M at these Q^2 values: significantly better than the global analysis of previous Rosenbluth measurements, and also more precise than the polarization transfer measurements below 3 GeV^2 .

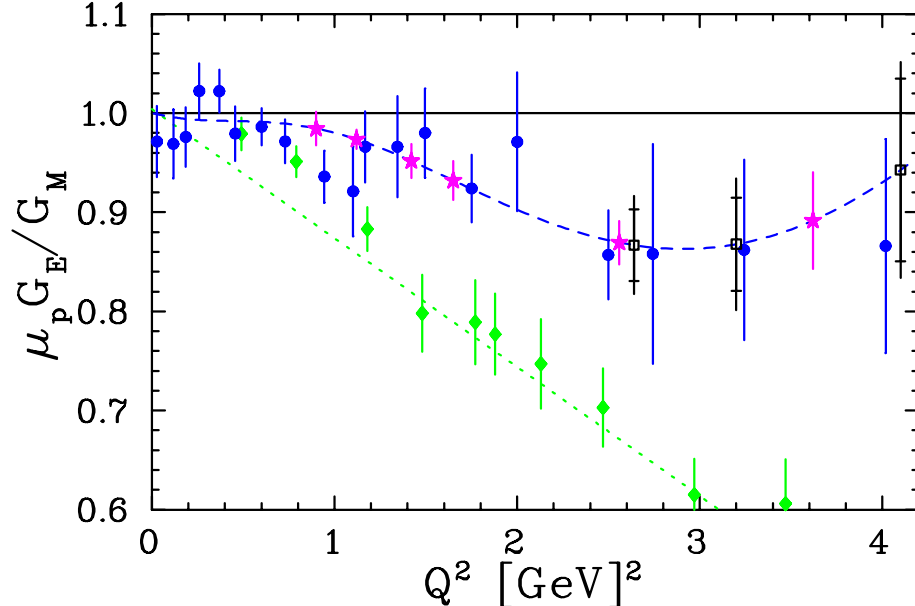


FIG. 11: $\mu_p G_E/G_M$ as deduced from polarization transfer (solid green diamonds) and a global analysis of L-T separation experiments [5] (solid blue circles). The open black squares indicate the present and projected uncertainties of E01-001 (outer and inner error bars), placed on the fit from the global L-T analysis. The magenta stars are the projected uncertainties for this proposal. Note that the low Q^2 polarization transfer data shown are from the unpublished final analysis [4], and so show the anticipated final uncertainties.

V. CONCLUSIONS

With 9 days of running, we will make a high precision test of the linearity of the Rosenbluth plot at two Q^2 values. Deviations from linearity would be a clear indication of deviation from the Rosenbluth formalism, and provide an additional way to constrain models of the two-photon exchange. Various calculations of the two-photon exchange corrections, small enough to be unobserved by previous measurements but large enough to explain the discrepancy between Rosenbluth and polarization transfer, yield nonlinearities which can be observed at the three standard deviation level at both Q^2 values.

In addition, high precision L-T separations of G_E/G_M can be performed at four additional Q^2 values, allowing precise extractions of G_E/G_M from 0.9–3.6 GeV^2 . Given a form for the two-photon exchange corrections, such high precision data can be compared to high precision polarization transfer data and used to extract the size of two-photon corrections. These data will also allow better tests of models of two-photon corrections which attempt to explain the discrepancy.

-
- [1] M. K. Jones et al., Phys. Rev. Lett. **84**, 1398 (2000).
 - [2] O. Gayou et al., Phys. Rev. Lett. **88**, 092301 (2002).
 - [3] O. Gayou et al., Phys. Rev. C **64**, 038202 (2001).
 - [4] V. Punjabi et al., (unpublished).

- [5] J. Arrington (2003), nucl-ex/0309011.
- [6] B. D. Milbrath et al., Phys. Rev. Lett. **82**, 2221(E) (1999).
- [7] D. Dutta et al. (2003), nucl-ex/0303011.
- [8] J. Arrington, Phys. Rev. **C68**, 034325 (2003).
- [9] J. Arrington, R. E. Segel, et al., Jefferson lab experiment E01-001.
- [10] P. A. M. Guichon and M. Vanderhaeghen, Phys. Rev. Lett. **91**, 142303 (2003).
- [11] E. J. Brash, A. Kozlov, S. Li, and G. M. Huber, Phys. Rev. C **65**, 051001 (2002).
- [12] D. Higinbotham, (unpublished).
- [13] P. G. Blunden, W. Melnitchouk, and J. A. Tjon, Phys. Rev. Lett. **91**, 142304 (2003).
- [14] M. P. Rekalo and E. Tomasi-Gustafsson (2003), nucl-th/0307066.
- [15] A. Afanasev, private communication.
- [16] L. W. Mo and Y.-S. Tsai, Rev. Mod. Phys. **41**, 205 (1969).
- [17] Y. S. Tsai, Tech. Rep., SLAC Report (1971).
- [18] N. Meister and D. Yennie, Phys. Rev. **130**, 1210 (1963).
- [19] J. Arrington (2003), nucl-ex/0311019.
- [20] L. Andivahis et al., Phys. Rev. D **50**, 5491 (1994).
- [21] R. C. Walker et al., Phys. Rev. D **49**, 5671 (1994).
- [22] M. E. Christy et al., (unpublished).
- [23] C. Berger, V. Burkert, G. Knop, B. Langenbeck, and K. Rith, Phys. Lett. B **35**, 87 (1971).
- [24] J. Mar et al., Phys. Rev. Lett. **21**, 482 (1968).
- [25] Y. S. Tsai, Phys. Rev. **122**, 1898 (1961).
- [26] R. L. Anderson, B. Borgia, G. L. Cassiday, J. W. DeWire, A. S. Ito, and E. C. Loh, Phys. Rev. **166**, 1336 (1968).
- [27] B. Bouquet, D. Benaksas, B. Grossetete, B. Jean-Marie, G. Parrou, J. P. Poux, and R. Tchapatian, Phys. Lett. **B26**, 178 (1968).
- [28] W. Bartel, B. Dudelzak, H. Krehbiel, J. M. McElroy, R. J. Morrison, W. Schmidt, V. Walther, and G. Weber, Phys. Lett. **B25**, 242 (1967).
- [29] R. L. Anderson, B. Borgia, G. L. Cassiday, J. W. DeWire, A. S. Ito, and E. C. Loh, Phys. Rev. Lett. **17**, 407 (1966).
- [30] A. Browman, F. Liu, and C. Schaerf, Phys. Rev. **139**, B1079 (1965).
- [31] D. Yount and J. Pine, Phys. Rev. **128**, 1842 (1962).
- [32] G. L. Cassiday, J. W. DeWire, H. Fischer, A. Ito, E. Loh, and J. Rutherford, Phys. Rev. Lett. **19**, 1191 (1967).
- [33] R. R. Lewis, Phys. Rev. **102**, 537 (1956).
- [34] S. D. Drell and M. Ruderman, Phys. Rev. **106**, 561 (1957).
- [35] S. D. Drell and S. Fubini, Phys. Rev. **113**, 741 (1959).
- [36] N. R. Werthammer and M. A. Ruderman, Phys. Rev. **123**, 1005 (1961).
- [37] G. K. Greenhut, Phys. Rev. **184**, 1860 (1969).
- [38] W. Melnitchouk, private communication.
- [39] A. Afanasev, I. Akushevich, and N. P. Merenkov (2002), hep-ph/0208260.
- [40] M. P. Rekalo and E. Tomasi-Gustafsson (2002), nucl-th/0202025.
- [41] D. Dutta, private communication.
- [42] C. E. Keppel et al., Jefferson lab experiment E94-110.